HHS Public Access

Author manuscript

J Biomater Sci Polym Ed. Author manuscript; available in PMC 2018 November 01.

Published in final edited form as:

J Biomater Sci Polym Ed. 2017 November ; 28(16): 1826–1846. doi:10.1080/09205063.2017.1354672.

Growth factor sequestration and enzyme-mediated release from genipin-crosslinked gelatin microspheres

Paul A. Turner, **Jeffrey S. Thiele**, and **Jan P. Stegemann**

Department of Biomedical Engineering, University of Michigan, Ann Arbor, MI, USA

Abstract

Controlled release of growth factors allows the efficient, localized, and temporally-optimized delivery of bioactive molecules to potentiate natural physiological processes. This concept has been applied to treatments for pathological states, including chronic degeneration, wound healing, and tissue regeneration. Peptide microspheres are particularly suited for this application because of their low cost, ease of manufacture, and interaction with natural remodeling processes active during healing. The present study characterizes gelatin microspheres for the entrapment and delivery of growth factors, with a focus on tailored protein affinity, loading capacity, and degradation-mediated release. Genipin crosslinking in PBS and CHES buffers produced average microsphere sizes ranging from 15 to 30 microns with population distributions ranging from about 15 to 60 microns. Microsphere formulations were chosen based on properties important for controlled transient and spatial delivery, including size, consistency, and stability. The microsphere charge affinity was found to be dependent on gelatin type, with *type A* (GelA) carriers consistently having a lower negative charge than equivalent *type B* (GelB) carriers. A higher degree of crosslinking, representative of primary amine consumption, resulted in a greater negative net charge. Gelatin type was found to be the strongest determinant of degradation, with GelA carriers degrading at *higher rates* versus similarly crosslinked GelB carriers. Growth factor release was shown to depend upon microsphere degradation by proteolytic enzymes, while microspheres in inert buffers showed long-term retention of growth factors. These studies illuminate fabrication and processing parameters that can be used to control spatial and temporal release of growth factors from gelatin-based microspheres.

Keywords

VEGF; BMP2; tissue engineering; microcarriers; cytokine delivery; controlled drug release

Introduction

Recent breakthroughs in understanding the diverse structure and roles of bioactive proteins have generated an increasing interest in controlling the localization and transient availability

CONTACT: Jan P. Stegemann jpsteg@umich.edu.

ORCID

Paul A. Turner http://orcid.org/0000-0001-9857-3541

Disclosure statement

No potential conflict of interest was reported by the authors.

of growth factors to control cell function and tissue development. Similar efforts have been made to apply lessons from natural physiological remodeling to improve the treatment of pathological states such as chronic degeneration, delayed wound healing, and fracture fixation. Tissue regeneration is a complex process that requires coordinated formation of new tissue, concomitant with generation of an integrated vasculature to supply nutrients and remove metabolic waste products. In large defects, regeneration may be limited by insufficient tissue formation and/or delayed vascularization [1], and therefore delivery of exogenous growth factors is an attractive approach to accelerate healing. However, global growth factor administration is costly, inefficient, and ineffective due to the short half-life and *limited* activity of these factors *in vivo* [2,3]. Furthermore, unmoderated growth factor administration can lead to anomalous and ectopic tissue formation [3]. For these reasons, spatially- and temporally-controlled release of growth factors is a promising approach to coordinating and enhancing tissue repair.

Hydrogel microcarriers have been used to sequester growth factors through stable electrostatic interactions between oppositely charged molecules, known as polyionic complexes [4,5]. This mechanism has been utilized to adsorb growth factors to polymeric carriers, including alginate [3,6], gelatin [4,7,8], polyanhydrides [9], and polyesters [10–12]. The release rate from such matrices is typically determined by the rate and degree of polymer swelling and degradation both *in vitro* and *in vivo* [4,7,13]. For peptide-based systems such as gelatin matrices, growth factor loading via electrostatic interaction is dependent on the isoelectric point (pI) of the carrier material relative to the growth factor of interest [14]; for example, negatively charged (pI < 7) materials are favored for delivery of positively charged (pI > 7) molecules under physiological conditions. Release is then dictated by the local ionic environment [4,8], peptide conformation [4,8], water absorption [14,15], and the degradation rate of the carrier material [4,14,15]. In such systems, short-term ‘burst’ release can be minimized by crosslinking the peptide using glutaraldehyde [14,15], carbodiimide (EDC) [16], or genipin [17–20]. Modulation of the crosslinking conditions can be used to tailor the properties of the peptide matrix, and such approaches have been shown to increase growth factor loading efficiency, decrease burst-release, and enable long-term growth factor retention.

Gelatin has been used widely for delivery of bioactive molecules, and a variety of growth factors have been adsorbed to gelatin-based matrices, including bFGF [4,7,8], BMP2 [4,15,21], *BMP4* [22], VEGF [4,15], and TGF-β [4,13,23], *IGF* [21,23], *and NGF* [4,13,24]. Gelatin microparticles possess particular functional and logistical benefits for controlled delivery of growth factors due to their small size and high surface area to volume ratio. The use of polyionic complexing, as opposed to covalent immobilization or physical entrapment, avoids the need to expose cells or cytokines to protein-denaturing organic solvents or treatments. Gelatin microcarriers loaded in such a way mimic the physiological process of extracellular matrix (ECM)-mediated sequestration of inactive growth factors, whose release naturally directs and coordinates tissue remodeling. The small size of the carriers allows minimally-invasive delivery to the desired site and makes controlled spatial delivery possible. Growth factor reservoirs may also protect the delivered molecule from proteolytic degradation and preserve its physiological function by excluding large proteolytic enzymes [9,11]. Since gelatin is a form of denatured collagen, it retains important functional

properties such as biocompatibility, cell-adhesive peptide sequences, and enzymatic degradability to cell-secreted matrix metalloproteinases (MMP). Two types of gelatin are commonly used: gelatin Type A (GelA), which is isolated through an acid-based process, and gelatin Type B (GelB), which is extracted under alkaline conditions. Basic (lyme) treatment hydrolyzes peptide bonds resulting in a higher density of carboxyl groups relative to the source collagen, yielding a material with a negative ionization potential. Conversely, acid treatment produces a gelatin with higher pI similar to native collagen. Additionally, treatment time may affect gelatin molecular weight, altering solution viscosity and gel viscoelastic response (bloom strength). Thus, gelatin processing influences both physical properties and electrochemical affinity.

Bone regeneration is an example application in which controlled release of multiple growth factors has been shown to improve outcomes [25–27]. Vascular endothelial growth factor (VEGF) released by supporting cells (e.g. MSC and fibroblasts) or by activated immune cells is associated with increased proliferation and differentiated functionality of endothelial cell populations, leading to angiogenesis and vasculogenesis [1,28,29]. Bone morphogenetic protein 2 (BMP2) is a potent agonist of mesenchymal osteogenesis [30], which has been used clinically to promote bone regeneration [31–33]. Ideally, growth factor release should be triggered by local, cell-mediated matrix remodeling to mimic the native healing process, allowing angiogenesis to precede osteogenesis, without causing ectopic tissue formation. Therefore, spatial and temporal control of VEGF and BMP2 delivery via degrading microsphere carriers may be an effective way to enhance osteoregenerative therapies.

In the present study, we developed and characterized gelatin-based microspheres reacted with genipin, a biocompatible and polymerizable crosslinker, which were designed for cell-controlled delivery of BMP2 and VEGF. Fabrication parameters were varied to tailor microsphere size and swelling, as well as protein affinity, loading potential, and degradation-mediated release. Particular emphasis was placed on the gelatin type and genipin crosslinking conditions, which were varied to tailor the properties of the resulting microspheres. Selected microsphere formulations were then exposed to proteolytic enzymes and the degradation rate and corresponding rate of BMP2 and VEGF release were characterized. The data demonstrate that gelatin microspheres can be made to respond to cell-initiated degradation, and their formulation can be tailored to provide some control over growth factor release. Such microspheres allow efficient, localized, and economical therapeutic delivery that may promote sustained and controlled tissue remodeling.

Materials and methods

Materials

Gelatin type A (porcine skin, 175 bloom) and type B (bovine skin, 225 bloom), and 2-(Cyclohexylamino)ethanesulfonic acid (CHES) were purchased from Sigma Aldrich (St. Louis, MO, USA). Polydimethylsiloxane (PDMS, 100 cSt) was purchased from Clearco Products (Bensalem, PA, USA). Pluronic® L101 was purchased from BASF Corporation (Vandalia, IL, USA). Genipin was purchased from Wako Chemicals (Richmond, VA, USA). Collagenase-II and CLSPA (purified) collagenase were purchased from Worthington Biochemical (Lakewood, NJ, USA). Recombinant human VEGF-165 (rhVEGFI) and

VEGF-specific sandwich ELISA assay kits were purchased from Thermo Scientific (Rockford, IL, USA). Recombinant human BMP2 (rHBMP2) and BMP2-specific sandwich ELISA assay kits were purchased from R&D Systems (Minneapolis, MN, USA).

Fabrication of gelatin microspheres

Gelatin microspheres were produced by water-in-oil emulsification shown in Figure 1(a) along with representative micrographs of washed microspheres prior to genipin crosslinking. Briefly, 6 mL of 6 wt% gel A or B solution warmed to 40 °C was added dropwise to 70 mL of warm (40 °C) PDMS oil. The mixture was stirred by a custom impeller at 2300 rpm for 5 min to disperse the aqueous (gelatin) phase into fine, microscale droplets within the oil phase. The emulsification was then rapidly cooled to 4 °C in an ice bath and stirred for an additional 30 min to set the gelatin microspheres. The emulsification was then washed with three cycles of PBS/0.01% L101 surfactant and centrifuged at 200 g to collect the microspheres and remove residual PDMS oil.

Crosslinking of gelatin microspheres using genipin

Chemical crosslinking imparts gelatin microspheres with a negative electrochemical potential promoting adsorption of positively charged proteins and allows microspheres to swell under physiological conditions without eroding (Figure 1(b)). Gelatin microspheres were crosslinked by reacting lysine residues on adjacent molecules with amine-reactive genipin as summarized in Figure 1(c). Briefly, genipin has been proposed to form crosslinks via a two-stage process involving (1) Attack by a primary ε-amine from lysine on the C3 carbon in genipin and (2) S_N2 nucleoplic substitution between another primary amine and a genipin ester [34]. However, more complex structures have been suggested involving dimeric [35–38], trimeric [36], and tetrameric [36] genipin crosslinks. Crosslinking was accomplished by suspending the washed microspheres in 3-fold excess volume of reaction buffer (PBS or 0.2 M CHES) containing 1.0 wt% genipin. Though ethanol mixtures are the most common crosslinking media, PBS and CHES buffers allowed the reaction pH to be controlled and stabilized while improving genipin solubility in an aqueous environment. The pH of the reaction buffer was set to 7 or 10 using 1.0 N NaOH or HCl. The crosslinking reaction was allowed to proceed at room temperature (below the gelation point for both gel A and B) for 24 h for GelA and 96 h for GelB to achieve complete and similar degrees of crosslinking [19]. Crosslinking times were kept consistent for buffer type and pH, though preliminary studies indicated complete (>90%) crosslinking efficacy was achieved in CHES buffer within 6 h (data not shown). After the crosslinking reaction, microspheres were washed in ethanol followed by deionized water to remove reactants and reaction buffer. Microspheres were frozen at −80 °C and freeze-dried to remove all residual water mass. Though gelatin itself shows faint autofluorescence, genipin crosslinking imparts a distinct response at the 590/620 Ex/Em wavelengths used to visualize sphere morphology and measure degraded microsphere mass. Uncrosslinked gelatin micrographs (Figure 1(a)) were collected using an inverted phase contrast microscope (Olympus). Optical sections of crosslinked microspheres (Figure 2(a)) and 3D reconstructions (Figure 6(a)) were collected with confocal microscopy (Nikon A1) and processed using NIS Elements viewer software (Nikon).

Measurement of swelling ratio

The amount of water absorbed by the crosslinked gelatin, or swelling ratio, was measured using cylindrical pucks (diameter ~5 mm) cast from gelatin stocks and crosslinked using the same treatment as microsphere carriers. Briefly, gelatin pucks were cast in cylindrical molds using 200 μL of 6.0 wt% gelatin solution set at 4 °C. The gelatin pucks were then removed from their molds and suspended in 600 μL excess volume of reaction buffer (PBS or 0.2 M CHES, pH 7.0 or 10.0) containing 1.0 wt% dissolved genipin and allowed to react until completion (24 h for GelA, 96 h for GelB). After the crosslinking reaction, gelatin samples were washed three times for one hour each in excess ethanol followed by two *one-hour* washes in DI water. Samples were swelled in excess DI water overnight at 37 °C prior to measurement. Sample pucks were gently dabbed dry and weighed to determine their swelled (hydrated) weight (M_S). Samples were frozen at −80 °C and lyophilized, then re-weighed to determine their dry mass (M_D). Swelling ratios were calculated with the following equation:

$$\text{Water content} = \frac{M_S - M_D}{M_S}$$

Determination of degree of crosslinking

Percent crosslinked or crosslinking efficacy was quantified by ninhydrin assay based on the proportion of primary amines consumed during the gelatin-genipin crosslinking reaction. Approximately 3 mg of lyophilized microspheres were swelled in 300 μL PBS for 1 h and sonicated at 20 W for 20 s prior to assay. A working assay solution was made by mixing equal volumes of stock Solution A containing 218.6 mM citric acid, 7.0 mM Tin(II) Chloride, and 0.4 M NaOH in DI water with Solution B containing 224.5 mM Ninhydrin dissolved in ethylene glycol monomethyl ether. 1 mL assay solution was added to each sample and briefly mixed by vortex. Samples were gently boiled on a heating block set to 120 °C for 25 min. After cooling to room temperature, samples were diluted 3-fold in 50%/50% DI water/isopropanol. Sample volumes of 200 μL were aliquoted and their absorbance at 570 nm was read on a plate reader (Biotek) in triplicate.

Particle size analysis

The relative size of swelled crosslinked gelatin microspheres was determined by laser diffraction using a particle analyzer (Mastersizer 2000, Malvern Instruments, Westborough MA). Samples were prepared by suspension in DI water at a concentration of 10 mg/mL and allowed to swell overnight prior to measurement. Samples were deflocculated by sonication at 20 W for 1 min of 20 s on/off cycles. Suspended microspheres were added to the sample reservoir stirring at 500 rpm and sonication at 20% until the laser obscuration reached at least 15%. Measurements assumed a default refractive index of 1.52 and solvent RI of 1.33.

Determination of zeta potential

Charge affinity as represented by the zeta potential of the microsphere carriers was determined using a zeta potential analyzer (Zetasizer Nano ZSP, Malvern Instruments, Westborough MA) by measuring suspended particle motion in response to an applied electrical field. Samples were prepared by suspending approximately 1 mg of microsphere

carriers in 1 mL of PBS. Microspheres were deflocculated by sonication at 20 W for 1 min of 20 s on/off cycles prior to measurement. Samples were transferred to DTS1070 capillary cells and zeta potentials measured. Instrument settings used the refractive index of protein (1.45) with PBS as a dispersant (RI 1.334), with measurements of electrophoretic mobility fit to the Smoluchowski Model. At least six measurements were taken per sample and crosslinking condition.

Enzyme-mediated microsphere degradation

Degradation progress, defined by solubilization of degradation particles, was tracked fluorometrically on a Synergy H1 plate reader (Biotek) using 590/620 excitation/emission (unique to genipin-gelatin reaction). To determine the relative enzymatic degradation rates of crosslinked gelatin microspheres, 1 mg of microsphere samples were suspended in 200 uL of PBS containing 0–25 U/mL collagenase II. The plate reader was set to maintain 37 °C and continually scan the samples wells at 20 min intervals. As degradation progressed, solubilized mass increased the intensity of fluorescent signal. Sample degradation time was defined as the time to reach a steady emission after exposure to collagenase. A calibration curve relating microsphere mass to fluorescent emission was constructed from degraded GelA and GelB (PBS 7) microspheres. The calibration curve was linear and indicated the technique was applicable to solubilized mass concentrations of approximately 0.1–0.5 μg/mL.

Genipin polymerization and gelatin microsphere crosslinking

Genipin has been found to spontaneously undergo ring-opening polymerization in basic pH buffered conditions [36], forming long chains of 7–88 members (1600–20,000 Da) as described in Figure 1(d). To investigate the potential impact of genipin polymerization on microsphere properties, 1 wt% genipin was dissolved in 0.2 M CHES at pH 10 and allowed to polymerize for 0 to 12 h at room temperature. GelB microspheres were then crosslinked with the crosslinked genipin solution as described previously at pH 10 in CHES buffer.

Growth factor loading and degradation-mediated release

Purified collagenase (CLSPA) was used to demonstrate degradation-mediated growth factor release, as collagenase-II was found to cause deterioration of VEGF and BMP2, indicated by a gradual reduction in signal strength from the ELISA assay over time by preliminary studies. Evaluated under the same conditions, CLSPA collagenase was found to degrade gelatin microspheres at a similar rate as Collagenase II without affecting growth factor response to ELISA assays. Due to the gradual degradation period (14–24 h) and compatibility with growth factor molecules, CLSPA collagenase (5.0 U/mL) was chosen to perform degradation of growth factor-loaded microspheres.

Gelatin type A and B microspheres crosslinked in PBS at pH 7 were chosen as carrier vehicles for growth factor sequestration and release experiments based on their distinct size distributions, zeta potentials, and degradation rates. For VEGF studies, microspheres were loaded by swelling overnight in PBS-Albumin (5 mg/mL) buffer containing 20 μg/mL VEGF165 using 10× excess solvent mass (10 μL/mg carrier), based on the previously measured swelling ratios of the microsphere carriers. Microspheres were loaded with 200 ng

VEGF/mg carrier and samples were suspended in PBS-albumin and sonified at 20 W for 40 s with two 20 s on/off cycles. Degradation was initiated by separating microsphere samples into 100 μg aliquots and suspending in 5.0 U/mL collagenase. Loading buffer lacking microsphere carriers (representing 100% release) served as a positive control to normalize VEGF release, and VEGF-loaded microspheres suspended in PBS-albumin without collagenase served as negative controls. VEGF release was determined using a sandwich ELISA kit (Fisher) following the manufacturer's suggested protocols. Absorbance of the chromophore was measured at 450 nm using a plate reader (Biotek) with readings corrected against 550 nm absorbance.

For BMP2 sequestration and release studies, gelatin type A and B microspheres crosslinked in PBS at pH 7 were loaded with growth by swelling overnight in PBS-Albumin (5.0 mg/mL) buffer containing 80 μg/mL BMP2 using 10× excess solvent mass (10 μL/mg carrier). Microspheres were loaded with 800 ng BMP2/mg carrier. Microsphere samples were suspended in PBS-albumin and sonicated at 20 W for 40 s with two 20 s on/off cycles. Degradation was initiated by separating microsphere samples into 100 μg aliquots and suspending in 5.0 U/mL collagenase. VEGF-loaded microspheres suspended in PBS-albumin without collagenase served as negative controls. GelA and GelB (Genipin, PBS 7). BMP2 release was determined using a sandwich ELISA kit (R&D Systems) following the manufacturer's suggested protocols. Absorbance of the chromophore was measured at 450 nm using a Biotek plate reader with readings corrected against 550 nm absorbance. Released growth factor mass was quantified based on a BMP2 standard provided with the ELISA assay kit.

Statistical analysis

Microsphere swelling ratios, zeta potentials, degradation rates, and loading/release rates are expressed as numerical mean ± 95% confidence intervals. Microsphere dimensions are expressed as numerical mean and volume-weighted mean with error bars representing the 90% population distributions. Swelling ratios (Figure 3(a)), zeta potentials (Figure 3(b) and 4(b)), and degradation rates (Figure 5(b)) were analyzed by one-way ANOVA and individual groups were compared with a Bonferroni post hoc test using RGui data analysis software. *P*-values of less than 0.05 between groups were considered statistically significant. Growth factor release relative to microsphere degradation is fit to second or third order polynomial curves.

Results and discussion

Physical and electrochemical properties of crosslinked microsphere carriers

Gelatin microspheres produced via emulsification were generally spheroidal and demonstrated consistent and uniform autofluorescence when imaged at 590/620 Ex/Em wavelengths (Figure 2(a)). The median diameter (m) of microspheres ranged from 15 to 35 microns, depending on gelatin type and crosslinking regime, with 90% population distributions ranging from about 15 to 65 microns (Figure 2(b)). For comparison, we also sized human umbilical vein endothelial cells (HUVEC) and human mesenchymal stem cells (MSC) and found them to be of uniform size, with diameters of 18 microns. The size of

microsphere carriers in relation to the size of cells is provided for scale and functionally relevant to ensure that the carriers are small enough to efficiently deliver their load in close proximity to the cells. Gelatin processing conditions (GelA vs. GelB) strongly influenced microsphere physical properties, with GelB spheres typically larger and more polydisperse than GelA spheres emulsified and crosslinked under the same conditions. GelB (225 bloom strength) may be inferred to possess a higher molecular weight than GelA (175 bloom strength) and greater solution viscosity, resulting in larger microspheres during the emulsification process. A main thrust of this study was to determine the effect of crosslinking conditions on the properties of the resulting microspheres. These microspheres exhibited diverse morphologies, ranging from large, amorphous, and fragmented (e.g. GelA PBS10, GelB CHES7) to relatively small and uniform (GelA PBS7, GelB CHES10) as shown in Figure 2(a). Crosslinking both gel types in PBS in an alkaline environment (pH 10) resulted in larger spheres with greater variability in size, which was correlated with greater swelling ratios, relative to those crosslinked at a neutral pH. Crosslinking with CHES buffer exhibited the opposite trend, with microspheres reacted at basic pH having more homogenous size distributions and smaller average sizes relative to those reacted at neutral pH. This outcome may reflect the pH selectivity of the buffers, with PBS being more stable ionizing environment around neutral pH, whereas CHES is a more stable basic buffer. The CHES buffer has also been observed to rapidly promote genipin polymerization and complete gelatin crosslinking relative to PBS.

Crosslinking imparts thermal phase stability to otherwise water-soluble gelatin at 37 °C, and the mesh size, swelling potential, and free volume are largely determined by the degree of crosslinking and crosslink length. Genipin was used as a crosslinker of gelatin in this study due to its biocompatibility relative to aldehyde crosslinkers [38,39] and chromatic properties [34,40]. The reactivity of genipin has been shown to be dependent on pH, and tends to undergo spontaneous polymerization at basic pH [36,41]. To maintain neutral (pH 7) and basic (pH 10) reaction conditions, we used both PBS and CHES buffers. Other strategies used to control hydrogel microsphere size include altering emulsification conditions such as impeller rotation speed [16,38], *surfactant concentration* [16], and oil viscosity [16]. However, we chose to isolate crosslinking condition as a determining factor for microsphere dimensions, with all Gel type A and B microspheres produced by the same emulsification technique.

The swelling ratio of microspheres depended on gelatin type and crosslinking conditions, as shown in Figure 3(a). The swelling ratio is indicative of the connectivity of the matrix mesh, and is also important in determining loading volumes of growth factor solutions that are appropriate for specific formulations of microsphere carriers. Crosslinked gelatin samples absorbed 10–25× excess water vs. dry weight, corresponding to a range of 0.9–0.96 swelling ratios, reflecting an open mesh structure and a large free volume for loading biomolecules, and the strong affinity of the gelatin matrix for hydration. PBS-crosslinked gels exhibited reduced swelling ratios (~0.9–0.92) relative to uncrosslinked controls (0.94) when crosslinked in PBS at pH 7, but similar ratios after crosslinking at pH 10. Gels crosslinked in CHES buffer indicated increased swelling (0.96) when crosslinked at pH 10. Though consistent with other reported trends associating hydrogel swelling ratio with crosslink pH [36], the greater swelling ratio in alkaline CHES seems to contradict the smaller sphere sizes

measured after crosslinking. This inconsistency may be due to differences in reaction kinetics due to the large volume used to determine swelling ratio excluding genipin migration relative to the high surface area microsphere carriers.

Since crosslinking limits molecular chain mobility during liquid absorption and swelling, higher crosslink densities have typically been associated with lower swelling ratios in hydrogel systems [17,20,21,42]. Similar gelatin hydrogel systems have been reported with substantially lower water absorption (1.5–6× hydrated mass; i.e. 0.6–0.83 swelling ratios) with similar degrees of crosslinking (>75%) [17,20,21,43]. However, these systems are often crosslinked as cast films [17] or lyophilized scaffolds [21,43] with higher mass density and closer molecular affiliation at the time of crosslinking. Also, swelled systems are commonly crosslinked in ethanol rather than an aqueous environment [20,44,45], which we have observed to result in hydrogel compaction. Thus, it follows that our crosslinking mechanism performed on hydrogels in fully swelled (6 wt%) and aqueous state largely maintain high swelling potentials (similar to uncrosslinked controls) even after crosslinking.

Charge affinity as represented by the zeta potential of crosslinked gelatin microspheres also varied by gelatin type and crosslinking condition (Figure 3(b)). These values were measured to assess the potential for the carriers to attract and form polyionic complexes with oppositely charged proteins and growth factors. The zeta potential was measured at 20 °C in PBS (pH 7.4) to approximate the ionic environment under physiological conditions. Uncrosslinked control spheres made from the source gelatin exhibited zeta potentials around −3 mV in PBS. Genipin-crosslinked GelA microspheres were found to have zeta potentials ranging from −5 to −6 mV, while crosslinked GelB microspheres were significantly more negatively charged, with potentials ranging from −8 to −11 mV. Crosslinking in CHES buffer promoted a greater degree of crosslinking, resulting in a greater negative net charge. Microsphere carriers crosslinked in CHES buffer possessed a relatively high charge affinity and high degree of crosslinking (shown as superimposed values in Figure 3(b)). However, initial studies demonstrated poor loading potential by CHES pH 10 carriers, attributed to the high degree of crosslinking.

The processing techniques used to extract gelatin have been tailored to yield materials with varying isoelectric points and charge affinities. Specifically, gelatins produced by acid-treatment (GelA) possess similar isoelectric points (pI > 7) as their collagen source material. In contrast, alkaline pre-treatment hydrolyzes asparagine and glutamine residues in collagen, producing a gelatin (GelB) with a higher concentration of carboxyl groups and negative net charge (pI < 7). Traditionally GelA has been proposed to deliver negatively charged proteins, whereas GelB has been used to adsorb positively charged proteins [4]. However, due to the consumption of primary amines during crosslinking and the addition of negatively charged genipin [20], both gel types in the current experiment have been altered to possess a negative net charge for attracting cationic growth factors. Other studies have reported similar zeta potentials of gelatin carriers ranging from −9 mV [16] to −13 mV [46] at physiological pH.

In neutral or acidic environments, genipin acts to crosslink peptides by forming short monomeric (shown in Figure 1(c)), dimeric, trimeric, or tetrameric bridges between adjacent aminated molecules [47]. However, in alkaline environments genipin undergoes ring-

opening and polymerization, resulting in crosslink bridges of 7–88 repeat units [36,41] as described in Figure 1(d). To investigate the potential effects of crosslink length on microsphere properties, genipin was allowed to polymerize in CHES at pH 10 for 0–12 h prior to being used to crosslinking gelatin. GelB microspheres were chosen for their small size and homogeneity, and were then crosslinked for 24 h in CHES buffer at pH 10 using the polymerized genipin. Size measurements of the microspheres after crosslinking showed a correlation between increased genipin polymerization time and larger microspheres, as shown in Figure 4(a). Unpolymerized genipin (0 h) produced microspheres with a median diameter of 14 μm with a population distribution ranging from 8.9 to 21.5 μm (0 h). Polymerization of genipin for 12 h resulted in an increase in median microsphere diameter to 30.9 μm and range of 17.6 to 52.1 μm (12 h). Polymerized genipin also affected the zeta potential of crosslinked gelatin (Figure 4(b)), with the indicated zeta potential becoming more highly negative as the genipin was increasingly polymerized. While larger carrier size was correlated with greater negative charge, ionizable hydroxyl groups from the polymerized genipin (Figure 1(d)) may be responsible for contributing to the changes in charge affinity. These data demonstrate that genipin polymerization can be used to increase the chain length of the crosslinker, providing a potential mechanism for increasing mesh size and free volume for growth factor delivery.

Enzyme-mediated degradation of microsphere carriers

Collagenase treatment of crosslinked gelatin carriers was used to mimic the *in vivo* process of matrix degradation. A variety of proteases targeting gelatin are secreted by cells during chemotaxis and extracellular matrix remodeling, including gelatinases (MMP2 and MMP9) [48–50]. The collagenase enzyme cleaves amide linkages within the recurring peptide motif QPQGLAK found in collagen and gelatin, a common site targeted by MMP2 and MMP9 activity [50]. Collagenase treatment of the gelatin microspheres resulted in gradual dissolution into the supernatant, though the degraded material continued to exhibit a characteristic fluorescent response (590 ex/620 em). Gelatin degradation time could therefore be tracked by measuring the level of fluorescence in the supernatant, and full degradation was defined as the time point at which the fluorescence level stopped increasing. Microsphere degradation curves were derived by normalizing fluorescent measurements to both the background (samples without collagenase representing 0% degradation) and the maximum / terminal fluorescent reading (representing 100% degradation) shown in Figure 5(a). Degradation rates of microspheres crosslinked in PBS were largely independent of the pH at which they were prepared, as shown in Figure 5(a), at both low (5 U/mL) and high (25 U/mL) collagenase concentrations. In contrast, microspheres crosslinked in CHES exhibited different degradation rates depending on the pH at which they were crosslinked. Notably, spheres crosslinked in CHES at pH 10 were found to resist collagenase treatment, a property attributed to the combined high degree of crosslinking and small hydrated sphere size, resulting in minimal free volume for protease infiltration and activation while microspheres crosslinked at pH 7 in CHES were significantly larger and degraded more rapidly in collagenase. Degradation rates were derived by best-fit correlation from the linear region of the degradation curves, typically representing 70–90% of the total fluorescent signal. Degradation rate comparisons, expressed as percent of degradation per hour (Figure 5(b)), showed that gelatin type was the strongest determinant of degradation rate, with GelA

microsphere carriers typically degrading more rapidly than similarly crosslinked GelB carriers. Based on the relative enzymatic degradation rates, gels crosslinked in PBS at pH 7 were chosen for subsequent growth factor release studies. These crosslinking conditions produced GelA microsphere carriers that degraded completely over about 14 h, and GelB carriers that degraded over about 24 h when treated with 5 U/mL collagenase.

Growth factor loading and degradation-mediated release

GelA and GelB microsphere delivery vehicles crosslinked in PBS at pH7 were chosen for growth factor loading and release experiments based on their distinct electronegative potentials (−5 and −9 mV, respectively) and on minimum size and variability, properties important for homogenous transient and spatial delivery. Histograms shown in Figure 6(b) describe the morphological differences between GelA and GelB carriers crosslinked in PBS at pH 7, with GelB microspheres skewed towards higher volumes (50% of the population volume in spheres larger than 22 μm, ū).

Cell-secreted MMPs, especially gelatinases (MMP2 and 9) released by MSC and endothelial cells, cause the release of matrix-bound VEGF to promote endothelial cell organization and angiogenesis [51,52]. GelA and GelB microspheres were loaded with VEGF and treated with collagenase to induce growth factor delivery, with release normalized to positive controls containing no microsphere carrier, as shown in Figure 7. GelA microspheres retained 56% of the loaded VEGF (110 ng/mg carrier), and released up to 76% (152 ng/mg carrier) over 12 h (90 ng burst + 62 ng due to degradation), (Figure 7(a)). GelB spheres retained 91% of loaded VEGF (182 ng/mg carrier), released up to 33% (66 ng/mg carrier) over 24 h (16 ng burst + 50 ng due to degradation), (Figure 7(a)). Thus, the more voluminous GelB carriers possessing greater negative charge showed greater VEGF retention (lower initial burst), but slower and overall less VEGF mass released due to degradation compared to GelA carriers (Figure 7(b)). VEGF release profiles were best fit to a third order polynomial model, with release skewed towards the degradation of the first 50% of the sphere mass. VEGF-loaded microspheres not exposed to collagenase were used as negative controls, and retained VEGF without significant release for 2 weeks in the absence of enzymatic degradation (Figure 7(c)). Nagai et al. (2010) previously demonstrated collagenase-mediated VEGF release from carbodiimide- crosslinked collagen microspheres, though their crosslinking formula produced positively-charged carriers. From our model microcarriers, degree of negative charge was demonstrated to be a predictor of VEGF loading and subsequent release characteristics.

BMP2 is a potent osteogenic mediator of the TGF family necessary for natural fracture repair [30]. It has been proposed that BMP2 activity *in vivo*, like VEGF, may be modulated by interaction with the extracellular matrix via proteoglycans such as heparan sulfate [53]. Similarly, our loading data demonstrated that BMP2 may associate with gelatin microcarriers, with loading capacity dependent upon gelatin type and negative charge of the carrier. In this experiment, GelA and GelB microspheres were loaded with 800 ng/mg BMP2 using a similar technique as with VEGF. BMP2 release was mediated by gelatin degradation initiated by 5 U/mL collagenase, as shown in Figure 8. GelA spheres retained ~75% of loaded BMP2 (~600 ng/mg carrier), while releasing up to ~80% (~640 ng/mg carrier) over

12 h (~200 ng burst + ~440 ng due to degradation), (Figure 8(a)). GelB spheres retained ~92% of loaded BMP2 (~736 ng/mg carrier) and subsequently released up to ~40% (~320 ng/mg carrier) over 24 h (64 ng burst + 256 ng due to degradation). Similar to the trends observed with VEGF, BMP2 loading was higher in GelB microspheres compared to GelA, though degradation-mediated gowth factor release was also incomplete from both carriers (ELISA indicated less than 100% of loaded mass) (Figure 8(b)). BMP2 release profiles were best fit to a second order polynomial model, though release appeared more gradual with respect to degradation compared to VEGF. GelA and GelB microspheres loaded with 400 ng BMP2 per mg carrier showed high (<90%) retention for 2 weeks while maintained in a PBS-albumin buffer (Figure 8(c)).

VEGF and BMP2 were released in conjunction with microcarrier degradation and solubilization. Previous studies [4,8] have investigated the effects of gelatin type on loading efficacy and release, with optimal outcomes generally achieved from matching acidic type B (negatively-charged) gelatin with basic (positively charged) growth factors. However, our methods for crosslinking with genipin induced a net negative charge from both gel types, with differences in degree that were dependent on gelatin type and crosslinking technique. The differences in loading and release rates of the growth factors may be attributed to the difference in zeta potentials of the carriers, as well as their relative degradation rates. GelA spheres showed overall less loading, but more efficient and effective (more complete) release with relatively faster degradation rates compared to the GelB carriers. VEGF release occurred in three distinct stages: initial (burst) release of unbound growth factor, rapid early degradation-mediated release, and slow late-stage release. Gelatin type and zeta potential determined the amount of growth factor retained by the microsphere carriers, with GelB carriers retaining approximately twice the mass of VEGF as equivalent GelA carriers. However, both carrier types showed similar degradation-mediated release, with 87% of the measured VEGF release from GelA occurring within the first 30% of solubilized microsphere mass, with 61% released by GelB for a similar degree of degradation. Both gelatin carriers showed growth factor retention in the absence of degradation. Like VEGF, BMP2 retention and burst release was determined by carrier type and zeta potential. However, BMP2 release was more consistent and sustained throughout the duration of degradation. Together, these results indicate the effect of matched electrochemical affinity on VEGF and BMP2 loading into gelatin carriers and subsequent release due to enzymatic degradation. Despite the apparent complete enzymatic degradation and solubilization of the gelatin hydrogel carriers, both systems (GelA and GelB) indicated incomplete growth factor release. This phenomenon has been documented for similar affinity-based delivery methods [4,13,22,23,54] and, as the total growth factor release in both systems is proportional to carrier zeta potential, may be attributed to the influence of growth factor-matrix affiliation on protein solubilization. This interaction may also result in steric hindrance interfering with antibody binding during the quantitative ELISA assay.

High crosslink density in hydrogels has been shown to increase protein retention and decrease the rate of long term release [14,15] due to limited free volume and physical restrictions on molecular mobility and diffusion. Though our system demonstrated similar high degrees of crosslinking for GelA and GelB carriers (73 and 82%, respectively) and high degrees of swelling (89 and 92%, respectively), carriers demonstrated differential loading

potentials relative to their charge affinity (−5 and −9 mV, respectively). After the initial burst-release of unbound growth factor, spontaneous release due to gradual diffusion, in the absence of degradation, was also found to be minimal with both GelA and GelB carriers. Other factors such as temperature [8], and solution ion concentration [8,46], pH [46], and may affect the conformation of the gelatin carrier or electrochemical affinity with loaded proteins. Microspheres were loaded overnight at 37 °C to maximize molecular mobility, optimizing swelling and growth factor uptake [8]. Loading was carried out in an aqueous environment (PBS) at physiological pH to maximize hydrogel swelling as a result of chain repulsion from high charge density from ionized carboxyl groups [46] which also attract and bind cationic growth factors. In this way, release experiments were designed to harness and optimize the factors affecting binding and release of growth factors from gelatin microsphere carriers based on the outcomes of previously published studies, resulting in an effective and efficient electrochemically-selective gelatin hydrogel delivery system.

The genipin-crosslinked gelatin microspheres address an ongoing need for efficient spatial and temporal control of growth factor delivery. Though our experimental design demonstrated VEGF and BMP2 sequestration and release, such a system may be appropriate for a variety of cationic growth factors such as PDGF, TGFβ, IGF, bFGF, and BMP4. There has been much recent interest in coordinated or sequential delivery of synergistic growth factors to direct tissue regeneration such as chondrogenesis (TGFβ/IGF) [23], osteogenesis (BMP2/IGF) [21], myocardial infarction (IGF/VEGF) [55], and angiogenesis (VEGF/PDGF) [56]. We propose that our results indicate potential application for sequential therapeutic delivery of VEGF and BMP2 to promote osteogenesis at an ischemic or critical-sized fracture defect site. In this case, GelA carriers have shown the potential to rapidly release loaded VEGF upon degradation to promote the migration and infiltration of endothelial cells. Slower-degrading GelB carriers may be used to gradually release BMP2, inducing osteogenic differentiation and calcification. Therefore, we propose that the results from this experiment may be used as a model to alter growth factor loading and release kinetics as needed for a variety of therapeutic applications.

Conclusions

We have demonstrated that the physical and electrochemical properties of microsphere carriers, specifically the size distribution, swelling ratio, and electrical affinity/zeta potential are dependent upon gelatin type, and may be manipulated by altering the crosslinking environment. Similarly, the rate of enzymatic degradation of the microsphere carriers may be altered by choice of gelatin type and crosslinking protocol. Loading potential of both rhVEGF165 and rhBMP2 were found to be dependent on growth factor chemistry and carrier zeta potential, with a higher loading rates correlated with greater negative charge. Finally, growth factor release was shown to depend upon microsphere degradation by proteolytic enzymes, while loaded microspheres in inert buffers showed long-term retention of growth factors. This work has potential impact in the design and implementation of biodegradable gelatin microspheres for local growth factor delivery where controlled dosage and release rates are important for clinical outcomes.

Acknowledgments

The authors would like to thank Dr. Joerg Lahann for access to analytical equipment (Mastersizer and Zetasizer), and Dr. Kathleen McEnnis for technical assistance. The content is solely the responsibility of the authors and does not necessarily represent the official views of the National Institutes of Health.

Funding

This work was supported in part by the National Institute of Arthritis and Musculoskeletal and Skin Diseases [grant number R01AR062636].

References

1. Hankenson KD, Dishowitz M, Gray C, et al. Angiogenesis in bone regeneration. Injury. 2011; 42:556–561. [PubMed: 21489534]
2. des Rieux A, Ucakar B, Mupendwa BPK, et al. 3D systems delivering VEGF to promote angiogenesis for tissue engineering. J Controlled Release. 2011; 150:272–278.
3. Poldervaart MT, Wang H, van der Stok J, et al. Sustained release of BMP-2 in bioprinted alginate for osteogenicity in mice and rats. PLoS One. 2013; 8:e72610. Epub 2013 Aug 27. [PubMed: 23977328]
4. Yamamoto M, Ikada Y, Tabata Y. Controlled release of growth factors based on biodegradation of gelatin hydrogel. J Biomater Sci Polym Ed. 2001; 12:77–88. Epub 2001 May 04. [PubMed: 11334191]
5. Young S, Wong M, Tabata Y, et al. Gelatin as a delivery vehicle for the controlled release of bioactive molecules. J Controlled Release. 2005; 109:256–274.
6. Gombotz WR, Wee SF. Protein release from alginate matrices. Adv Drug Deliv Rev. 2012; 64:194–205.
7. Tabata Y, Nagano A, Ikada Y. Biodegradation of hydrogel carrier incorporating fibroblast growth factor. Tissue Eng. 1999; 5:127–138. Epub 1999 Jun 08. [PubMed: 10358220]
8. Tabata Y, Nagano A, Muniruzzaman M, et al. In vitro sorption and desorption of basic fibroblast growth factor from biodegradable hydrogels. Biomaterials. 1998; 19:1781–1789. Epub 1998 Dec 18. [PubMed: 9856589]
9. Tabata Y, Gutta S, Langer R. Controlled delivery systems for proteins using polyanhydride microspheres. Pharm Res. 1993; 10:487–496. Epub 1993 Apr 01. [PubMed: 8483830]
10. Kanczler JM, Ginty PJ, Barry JJA, et al. The effect of mesenchymal populations and vascular endothelial growth factor delivered from biodegradable polymer scaffolds on bone formation. Biomaterials. 2008; 29:1892–1900. [PubMed: 18234329]
11. Cohen S, Yoshioka T, Lucarelli M, et al. Controlled delivery systems for proteins based on poly(lactic/glycolic acid) microspheres. Pharm Res. 1991; 08:713–720. Epub 1991 Jun 01.
12. Richardson TP, Peters MC, Ennett AB, et al. Polymeric system for dual growth factor delivery. Nat Biotechnol. 2001; 19:1029–1034. Epub 2001 Nov 02. [PubMed: 11689847]
13. Holland TA, Tabata Y, Mikos AG. In vitro release of transforming growth factor-beta 1 from gelatin microparticles encapsulated in biodegradable, injectable oligo(poly(ethylene glycol) fumarate) hydrogels. J Controlled Release. 2003; 91:299–313. Epub 2003 Aug 23.
14. Iwanaga K, Yabuta T, Kakemi M, et al. Usefulness of microspheres composed of gelatin with various cross-linking density. J Microencapsul. 2003; 20:767–776. Epub 2003 Nov 05. [PubMed: 14594665]
15. Patel ZS, Yamamoto M, Ueda H, et al. Biodegradable gelatin microparticles as delivery systems for the controlled release of bone morphogenetic protein-2. Acta Biomater. 2008; 4:1126–1138. Epub 2008 May 14. [PubMed: 18474452]
16. Nagai N, Kumasaka N, Kawashima T, et al. Preparation and characterization of collagen microspheres for sustained release of VEGF. J Mater Sci Mater Med. 2010; 21:1891–1898. Epub 2010 Mar 17. [PubMed: 20232232]
17. Bigi A, Cojazzi G, Panzavolta S, et al. Stabilization of gelatin films by crosslinking with genipin. Biomaterials. 2002; 23:4827–4832. Epub 2002 Oct 04. [PubMed: 12361622]

18. Huang KS, Lu K, Yeh CS, et al. Microfluidic controlling monodisperse microdroplet for 5-fluorouracil loaded genipin-gelatin microcapsules. J Controlled Release. 2009; 137:15–19. Epub 2009 Mar 07.
19. Solorio L, Zwolinski C, Lund AW, et al. Gelatin microspheres crosslinked with genipin for local delivery of growth factors. J Tissue Eng Regen Med. 2010; 4:514–523. Epub 2010 Sep 28. [PubMed: 20872738]
20. Yao C-H, Liu B-S, Chang C-J, et al. Preparation of networks of gelatin and genipin as degradable biomaterials. Mater Chem Phys. 2004; 83:204–208.
21. Kim S, Kang Y, Krueger CA, et al. Sequential delivery of BMP-2 and IGF-1 using a chitosan gel with gelatin microspheres enhances early osteoblastic differentiation. Acta Biomater. 2012; 8:1768–1777. Epub 2012 Feb 02. [PubMed: 22293583]
22. Nguyen AH, McKinney J, Miller T, et al. Gelatin methacrylate microspheres for controlled growth factor release. Acta Biomater. 2015; 13:101–110. [PubMed: 25463489]
23. Holland TA, Bodde EW, Cuijpers VM, et al. Degradable hydrogel scaffolds for *in vivo* delivery of single and dual growth factors in cartilage repair. Osteoarthritis and Cartilage. 2007; 15:187–197. Epub 2006 Sep 13. [PubMed: 16965923]
24. Chang CJ. Effects of nerve growth factor from genipin-crosslinked gelatin in polycaprolactone conduit on peripheral nerve regeneration-In vitro and *in vivo*. J Biomed Mater Res Part A. 2009; 91A:586–596. Epub 2008 Nov 06.
25. Kempen DHR, Lu L, Heijink A, et al. Effect of local sequential VEGF and BMP-2 delivery on ectopic and orthotopic bone regeneration. Biomaterials. 2009; 30:2816–2825. [PubMed: 19232714]
26. Lin Z, Wang J-S, Lin L, et al. Effects of BMP2 and VEGF165 on the osteogenic differentiation of rat bone marrow-derived mesenchymal stem cells. Exp Ther Med. 2014; 7:625–629. [PubMed: 24520257]
27. Peng H, Usas A, Olshanski A, et al. VEGF improves, whereas sFlt1 inhibits, BMP2-induced bone formation and bone healing through modulation of angiogenesis. J Bone Miner Res. 2005; 20:2017–2027. Epub 2005 Oct 20. [PubMed: 16234975]
28. Thomas KA. Vascular Endothelial growth factor, a potent and selective angiogenic agent. J Biol Chem. 1996; 271:603–606. [PubMed: 8557658]
29. Unemori EN, Ferrara N, Bauer EA, et al. Vascular endothelial growth factor induces interstitial collagenase expression in human endothelial cells. J Cell Physiol. 1992; 153:557–562. [PubMed: 1447317]
30. Tsuji K, Bandyopadhyay A, Harfe BD, et al. BMP2 activity, although dispensable for bone formation, is required for the initiation of fracture healing. Nat Genet. 2006; 38:1424–1429. Epub 2006 Nov 14. [PubMed: 17099713]
31. Balseiro S, Nottmeier EW. Vertebral osteolysis originating from subchondral cyst end plate defects in transforaminal lumbar interbody fusion using rhBMP-2. Report of two cases. Spine J. 2010; 10:e6–e10.
32. Lewandrowski K-U, Nanson C, Calderon R. Vertebral osteolysis after posterior interbody lumbar fusion with recombinant human bone morphogenetic protein 2: A report of five cases. Spine J. 2007; 7:609–614. [PubMed: 17526434]
33. Wong DA, Kumar A, Jatana S, et al. Neurologic impairment from ectopic bone in the lumbar canal: a potential complication of off-label PLIF/TLIF use of bone morphogenetic protein-2 (BMP-2). Spine J. 2008; 8:1011–1018. [PubMed: 18037352]
34. Butler MF, Ng Y-F, Pudney PDA. Mechanism and kinetics of the crosslinking reaction between biopolymers containing primary amine groups and genipin. J Polym Sci, Part A: Polym Chem. 2003; 41:3941–3953.
35. Lai JY, Li YT, Wang TP. In vitro response of retinal pigment epithelial cells exposed to chitosan materials prepared with different cross-linkers. Int J Mol Sci. 2010; 11:5256–5272. Epub 2010 Jan 01. [PubMed: 21614206]
36. Mi F-L, Shyu S-S, Peng C-K. Characterization of ring-opening polymerization of genipin and pH-dependent cross-linking reactions between chitosan and genipin. J Polym Sci, Part A: Polym Chem. 2005; 43:1985–2000.

37. Sundararaghavan HG, Monteiro GA, Lapin NA, et al. Genipin-induced changes in collagen gels: Correlation of mechanical properties to fluorescence. J Biomed Mater Res Part A. 2008; 87A:308–320. Epub 2008 Jan 09.
38. Wang L, Wang Y, Qu J, et al. The cytocompatibility of genipin-crosslinked silk fibroin films. J Biomater Nanobiotechnol. 2013; 04:213–221.
39. Sung HW, Huang RN, Huang LL, et al. In vitro evaluation of cytotoxicity of a naturally occurring cross-linking reagent for biological tissue fixation. J Biomater Sci Polym Ed. 1999; 10:63–78. Epub 1999 Mar 26. [PubMed: 10091923]
40. Qiu J, Li J, Wang G, et al. In vitro investigation on the biodegradability and biocompatibility of genipin cross-linked porcine acellular dermal matrix with intrinsic fluorescence. ACS Appl Mater Interfaces. 2013; 5:344–350. [PubMed: 23245190]
41. Mu C, Zhang K, Lin W, et al. Ring-opening polymerization of genipin and its long-range crosslinking effect on collagen hydrogel. J Biomed Mater Res Part A. 2013; 101A:385–393. Epub 2012 Aug 01.
42. Kirchmajer DM, Watson CA, Ranson M, et al. Panhuis Mih. Gelapin, a degradable g.enipin cross-linked gelatin hydrogel. RSC Adv. 2013; 3:1073–1081.
43. Lien S-M, Li W-T, Huang T-J. Genipin-crosslinked gelatin scaffolds for articular cartilage tissue engineering with a novel crosslinking method. Mater Sci Eng C. 2008; 28:36–43.
44. Lau TT, Wang C, Wang D-A. Cell delivery with genipin crosslinked gelatin microspheres in hydrogel/microcarrier composite. Compos Sci Technol. 2010; 70:1909–1914.
45. Liang HC, Chang WH, Lin KJ, et al. Genipin-crosslinked gelatin microspheres as a drug carrier for intramuscular administration:In vitro andin vivo studies. J Biomed Mater Res. 2003; 65A:271–282. Epub 2003 May 08.
46. Wang A, Cui Y, Li J, et al. Fabrication of gelatin microgels by a “cast” strategy for controlled drug release. Adv Func Mater. 2012; 22:2673–2681.
47. Mi F-L, Sung H-W, Shyu S-S. Synthesis and characterization of a novel chitosan-based network prepared using naturally occurring crosslinker. J Polym Sci, Part A: Polym Chem. 2000; 38:2804–2814.
48. Chen Q, Jin M, Yang F, et al. Matrix metalloproteinases: inflammatory regulators of cell behaviors in vascular formation and remodeling. Mediators Inflamm. 2013; 2013:928315. Epub 2013 Jul 11. [PubMed: 23840100]
49. Rundhaug JE. Matrix metalloproteinases and angiogenesis. J Cell Mol Med. 2005; 9:267–285. Epub 2005 Jun 21. [PubMed: 15963249]
50. Fonseca KB, Granja PL, Barrias CC. Engineering proteolytically-degradable artificial extracellular matrices. Prog Polym Sci. 2014; 39:2010–2029.
51. Egeblad M, Werb Z. New functions for the matrix metalloproteinases in cancer progression. Nat Rev Cancer. 2002; 2:161–174. Epub 2002 May 07. [PubMed: 11990853]
52. Ghajar CM, George SC, Putnam AJ. Matrix metalloproteinase control of capillary morphogenesis. Crit Rev Eukaryot Gene Expr. 2008; 18:251–278. Epub 2008 Jun 11. [PubMed: 18540825]
53. Ohkawara B, Iemura S, ten Dijke P, et al. Action range of BMP is defined by its N-terminal basic amino acid core. Curr Biol. 2002; 12:205–209. Epub 2002 Feb 13. [PubMed: 11839272]
54. Yao C, Roderfeld M, Rath T, et al. The impact of proteinase-induced matrix degradation on the release of VEGF from heparinized collagen matrices. Biomaterials. 2006; 27:1608–1616. [PubMed: 16183114]
55. Cittadini A, Monti MG, Petrillo V, et al. Complementary therapeutic effects of dual delivery of insulin-like growth factor-1 and vascular endothelial growth factor by gelatin microspheres in experimental heart failure. Eur J Heart Fail. 2011; 13:1264–1274. Epub 2011 Nov 03. [PubMed: 22045926]
56. Chen RR, Silva EA, Yuen WW, et al. Spatio–temporal VEGF and PDGF delivery patterns blood vessel formation and maturation. Pharm Res. 2007; 24:258–264. [PubMed: 17191092]

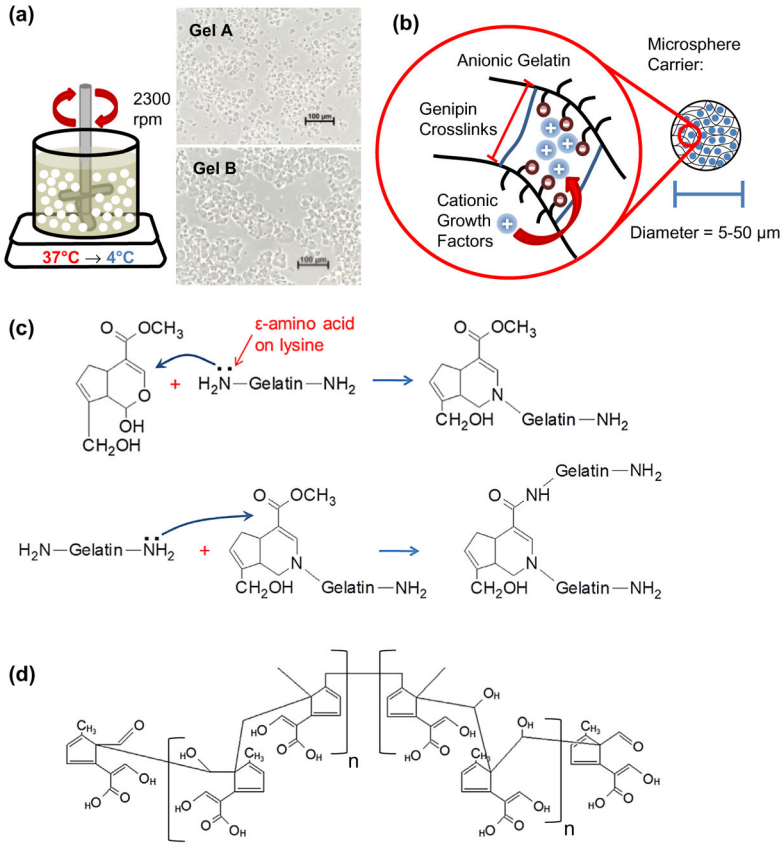

Figure 1.

Gelatin microsphere emulsification, crosslinking, and growth factor loading. (a) Schematic of the gel emulsification technique used to produce gelatin microspheres. Insets show microspheres made from gelatin Type A and gelatin Type B prior to crosslinking. (b) Schematic of genipin crosslinking of the gelatin matrix and the resulting mesh size and charge affinity. Cationic growth factors can bind to the anionic gelatin via electrostatic interactions. (c) Crosslink mechanism described by Butler, Ng, and Pudney (2003) showing reactivity of genipin with lysine primary amines found in gelatin. (d) Structure of genipin polymer proposed by Mi, Shyu, and Peng (2005) after undergoing ring-opening polymerization at basic pH.

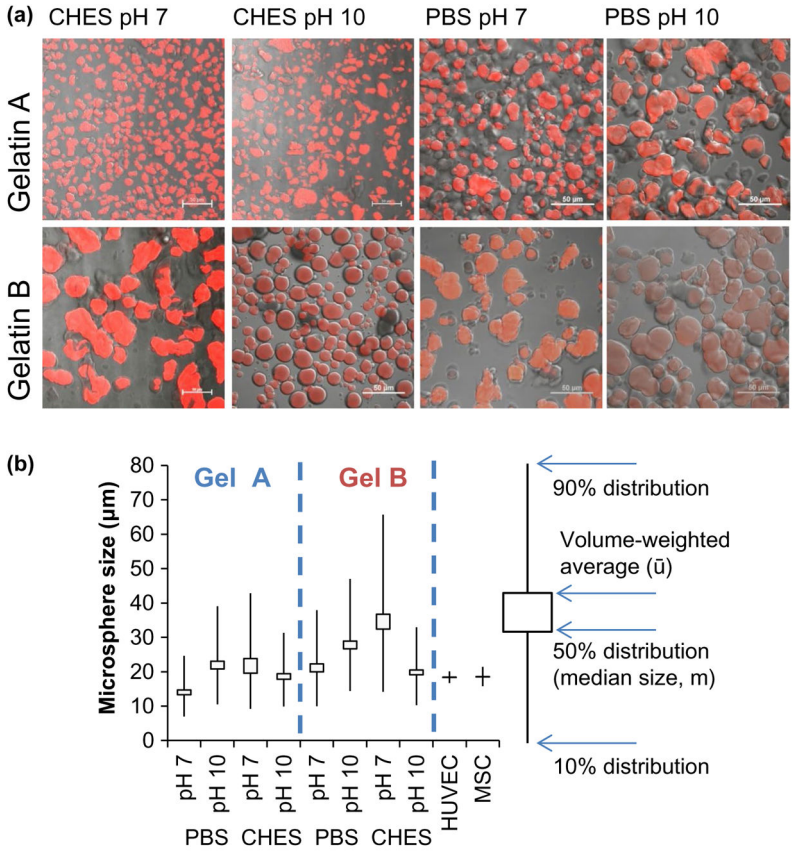

Figure 2.

Micrographs and size (b) measurements of crosslinked gelatin microsphere carriers. (a) Overlays of brightfield and fluorescent confocal microscopy sections of autofluorescent crosslinked gelatin microspheres. (b) Swelled microsphere dimensions in deionized water at room temperature. Box plots describe size distributions and median carrier diameter as a function of crosslinking regimen.

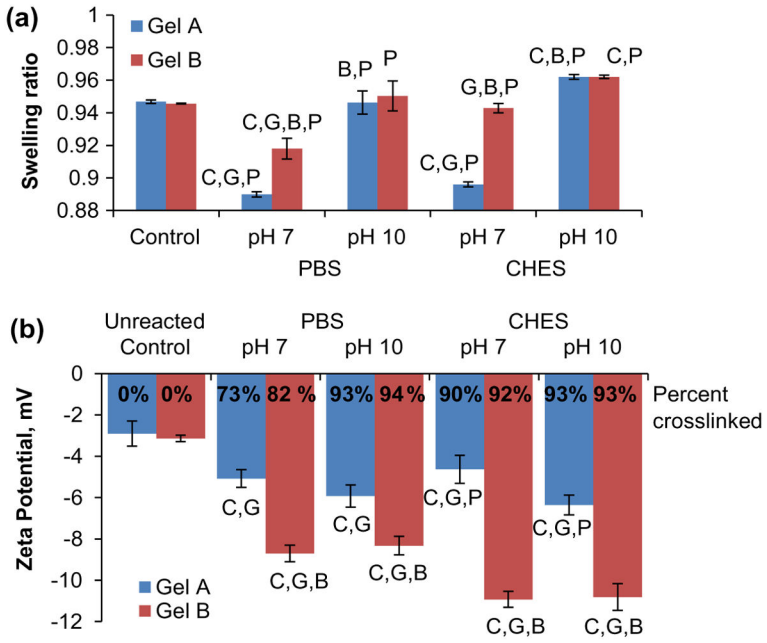

Figure 3.

Physiochemical characterization of gelatin microsphere carriers. (a) Swelling ratio measurements of crosslinked gelatin. (b) Zeta potentials and degree of crosslinking of gelatin and genipincrosslinked gelatin microsphere carriers. In both panels letters denote statistical significance ($p < 0.05$) between groups relative to control (C) or based on gel type (G), buffer type (B), or reaction pH (P).

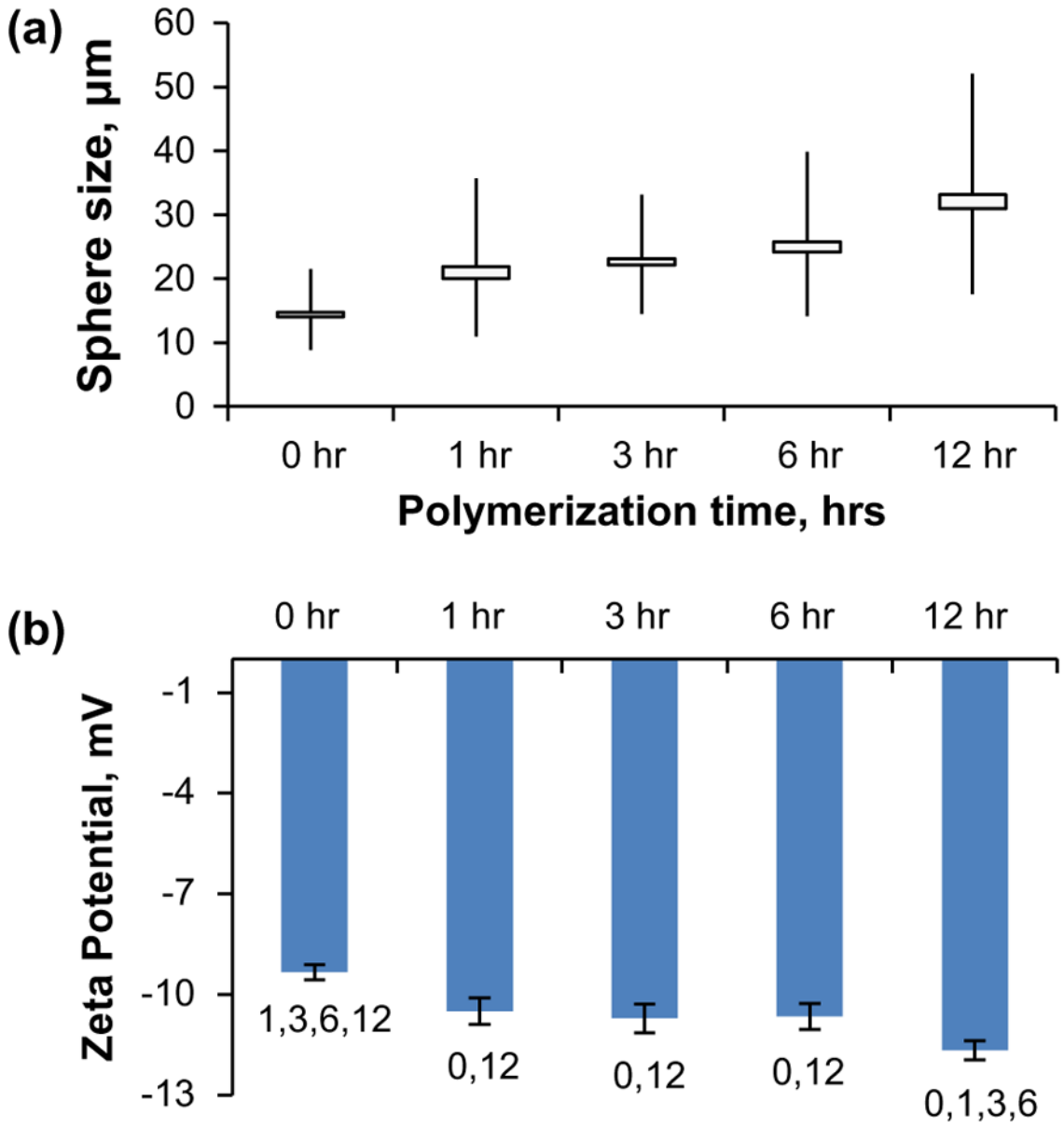

Figure 4.

Physiochemical characterization of GelB microsphere carriers crosslinked with polymerized genipin. (a) Size of GelB microspheres after crosslinking with genipin polymerized for 0–12 h at pH 10. (b) Zeta potentials of GelB microspheres after crosslinking with genipin polymerized for 0–12 h at pH 10. Numbers denote statistical significance ($p < 0.05$) between groups.

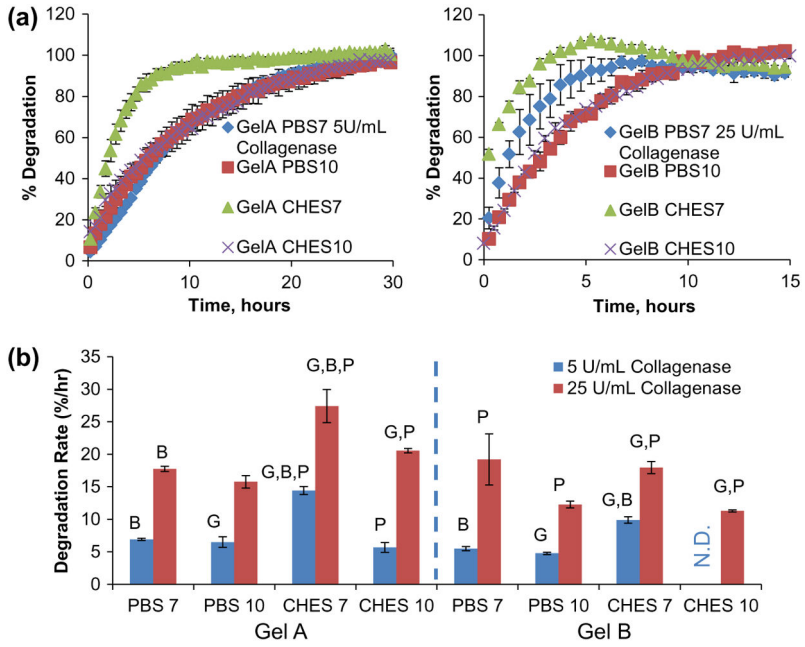

Figure 5.

Enzyme-mediated degradation of gelatin microsphere carriers. (a) Degradation curves generated from fluorescence emissions measured from microsphere samples exposed to low (5 U/mL) and high (25 U/mL) collagenase-II concentrations and (b) average degradation rates calculated from degradation curves. Letters denote statistical significance ($p < 0.05$) between groups based on gel type (G), buffer type (B), or reaction pH (P).

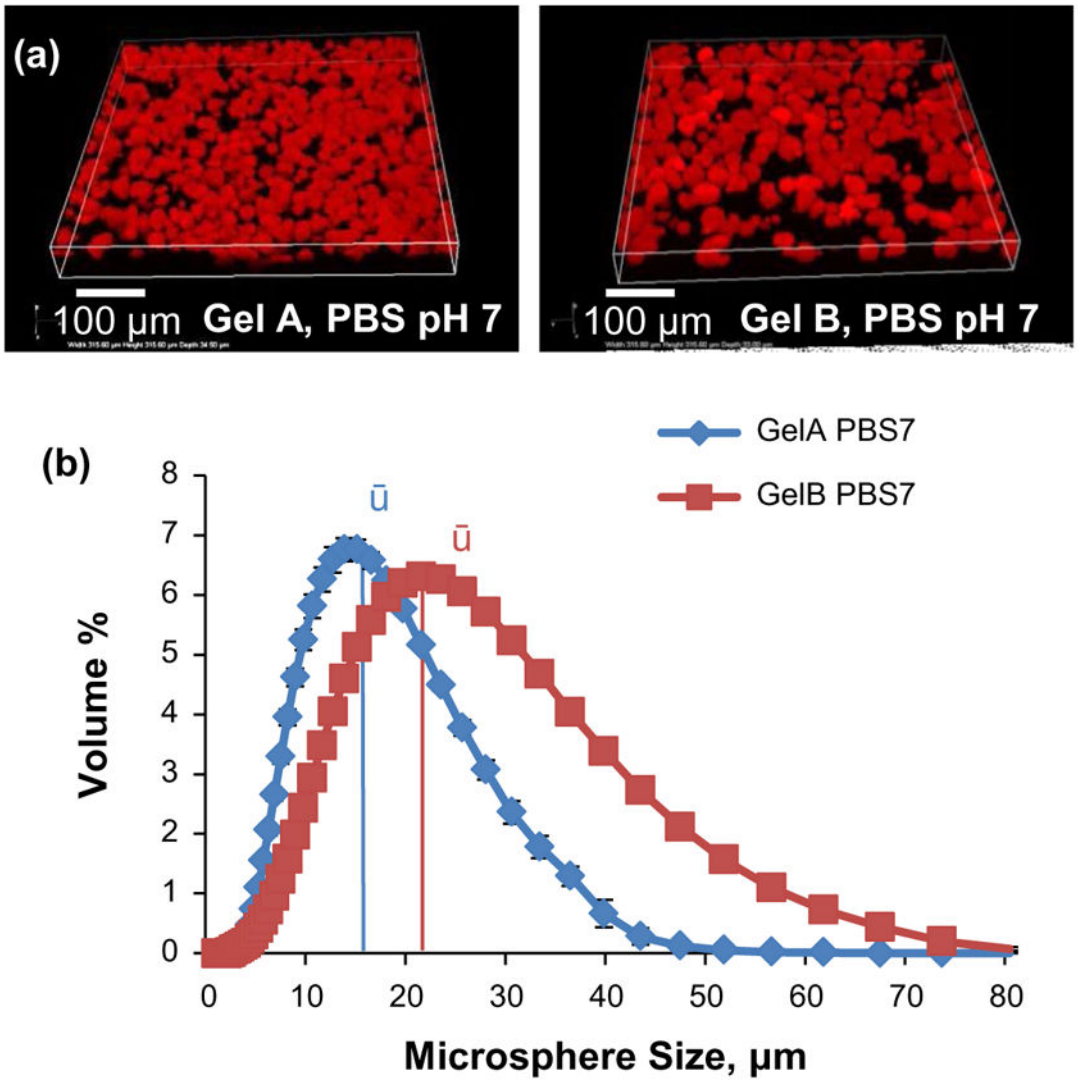

Figure 6.

Size measurements of crosslinked gelatin microsphere carriers. (a) Confocal 3-D reconstructions of autofluorescent gelatin microspheres. (b) Population histograms of GelA and GelB microspheres.

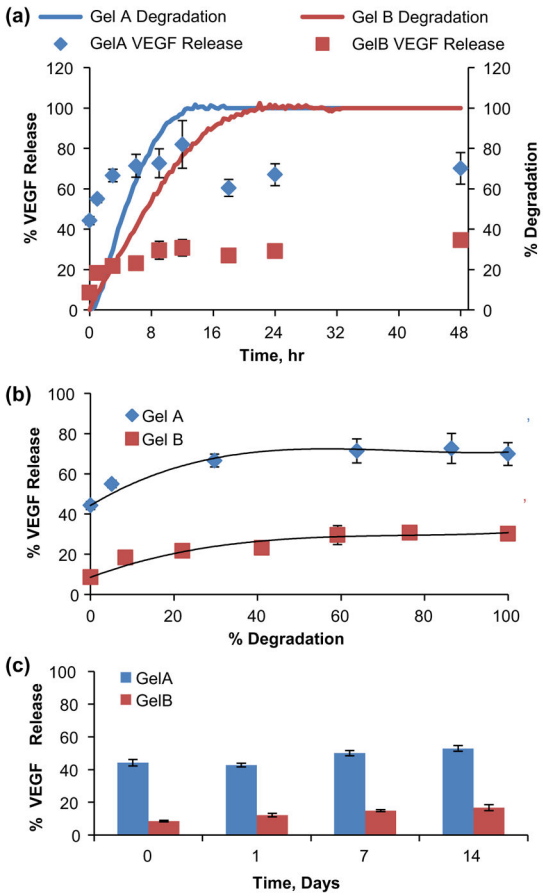

Figure 7.

Transient and degradation-mediated VEGF release from gelatin microsphere carriers. (a) Transient VEGF release from crosslinked gelatin microspheres overlayed against microsphere degradation profiles. (b) VEGF release modeled as a function of microsphere carrier degradation. (c) VEGF retained in the absence of enzymatic degradation.

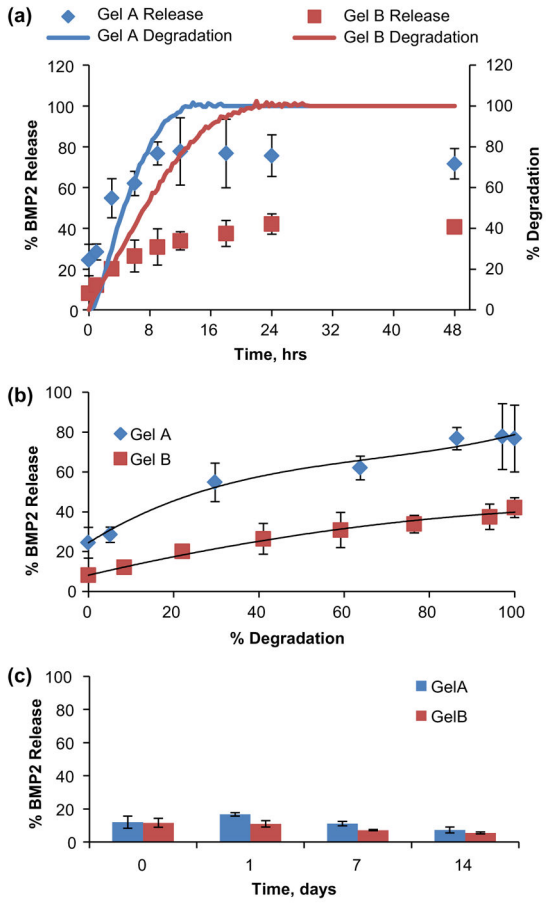

Figure 8.

Transient and degradation-mediated BMP2 release from gelatin microsphere carriers. (a) Transient BMP2 release from crosslinked gelatin microspheres overlayed against microsphere degradation profiles. (b) BMP2 release modeled as a function of microsphere carrier degradation. (c) BMP2 retained in the absence of enzymatic degradation.